
Research Article

Drug-Loaded Zein Nanofibers Prepared Using a Modified Coaxial Electrospinning Process

Weidong Huang,^{1,2,3} Tao Zou,¹ Shengfang Li,¹ Jinqiu Jing,^{1,2} Xianyou Xia,¹ and Xianli Liu²

Received 1 November 2012; accepted 4 March 2013; published online 21 March 2013

Abstract. This study investigated the preparation of drug-loaded fibers using a modified coaxial electrospinning process, in which only unspinnable solvent was used as sheath fluid. With zein/ibuprofen (IBU) co-dissolving solution and *N,N*-dimethylformamide as core and sheath fluids, respectively, the drug-loaded zein fibers could be generated continuously and smoothly without any clogging of the spinneret. Field emission scanning electron microscopy and transmission electron microscopy observations demonstrated that the fibers had ribbon morphology with a smooth surface. Their average diameters were 0.94 ± 0.34 and 0.67 ± 0.21 μm when the sheath-to-core flow rate ratios were taken as 0.11 and 0.25, respectively. X-ray diffraction and differential scanning calorimetry verified that IBU was in an amorphous state in all fiber composites. Fourier transform infrared spectra showed that zein had good compatibility with IBU owing to hydrogen bonding. *In vitro* dissolution tests showed that all the fibers could provide sustained drug release files via a typical Fickian diffusion mechanism. The modified coaxial electrospinning process reported here can expand the capability of electrospinning in generating fibers and provides a new manner for developing novel drug delivery systems.

KEYWORDS: coaxial electrospinning; drug-loaded fibers; sheath solvent; sustained release; zein.

INTRODUCTION

Electrospinning is a popular procedure for producing nanofibers due to ease of implementation and cost-effectiveness of the process and the unique properties and versatile applications of the resultant nanofibers (1–6). For pharmaceutical applications, electrospun polymer-based fibers have been investigated for providing different types of controlled drug release profiles, such as immediate, pulsatile, delayed, sustained, and biphasic releases (7–10). Among them, sustained drug release is gaining considerable attention as a method of administering and maintaining desired drug concentrations in the blood within a specified therapeutic window, or in target tissues within a desired duration of drug delivery (11–13).

However, for smooth preparation of drug-loaded polymer nanofibers with desired drug sustained release profiles, several concerns must be resolved. First, the polymer should have fine filament-forming property in a certain solvent under the electrical field, *i.e.* have good electrospinnability. Second, the host polymer matrix must be biocompatible for biomedical applications and meanwhile should be compatible with the guest active pharmaceutical ingredients. Third, the solvents

for preparing the spinning solutions should not only dissolve a certain amount of drug and polymer in the working solution for efficacious drug content and enough polymer chain-entanglement density necessary to prevent capillary breakup and Rayleigh instability for generating nanofibers with uniform structure but should also make the working solution amicable to the electrospinning process. However, a common failure example of preparing drug-loaded fibers using traditional single fluid electrospinning is the frequent clogging of the spinneret, often thought to be a result of high concentration of polymer in the solutions and/or high volatility of employed solvents (14–17).

Coaxial electrospinning, in which a concentric spinneret can accommodate two different liquids, is regarded as one of the most significant breakthroughs in this area (18). It has been applied broadly in controlling secondary structures of nanofibers, encapsulating drugs or biological agents into the polymer nanofibers, enclosing functional liquids within the fiber matrix, manipulating the size of self-assembled nanoparticles, preparing ultrafine fibers from concentrated polymer solutions previously thought to be unspinnable, and improving nanofibers' quality systematically (19, 20). Coaxial electrospinning is able to expand the capability of electrospinning in fabricating nanofibers in two manners. The first one is that it can prepare nanofibers from materials that lack filament-forming properties using traditional coaxial electrospinning process, where the sheath fluid often has good electrospinnability while the core fluid is unelectrospinnable (21–23). The second one is a modified coaxial electrospinning process first reported by Yu *et al.* (24, 25), where only unspinnable solvent is employed as sheath fluid. Through replacing the

¹ School of Chemical and Materials Engineering, Hubei Polytechnic University, 16 North Guilin Road, Huangshi, 435003, China.

² Hubei Key Laboratory of Mine Environmental Pollution Control and Remediation, Huangshi, 435003, China.

³ To whom correspondence should be addressed. (e-mail: weydong@163.com; ehda2012@126.com)

traditional interface between polymer jets and atmosphere partially by the interface between polymer jets and sheath solvents, the modified coaxial electrospinning opens a new way for generating nanofibers from polymer solutions. The modified coaxial process has been demonstrated to be a useful tool in preventing clogging of spinneret for continuous preparation of pure polymer nanofibers such as polyvinylpyrrolidone and polyacrylonitrile (24–26).

Zein is a mixture of proteins with different molecular weights in corn gluten. Apart from biodegradability and biocompatibility, zein has low hydrophilicity, high elasticity, and film-forming capabilities (27, 28). Zein is used to manufacture a wide variety of commercial products, including coatings for food, excipients in pharmaceuticals, and clothing. Recently, the electrospinning of zein into nanofiber mats for various applications, particularly in the biomedical field such as being a scaffold and matrix of novel drug delivery systems, has drawn increased attention (29–32). However, the electrospinning of zein is easily hindered by spinneret clogging. Kanjanapongkul *et al.* (16) reported that clogging would occur even when the zein concentration in its ethanol aqueous solutions (85 wt.%) decreased from an electrospinning level to electrospraying level (<18 wt.%).

In the present study, using *N,N*-dimethylformamide (DMF; boiling point, 153°C) as sheath fluid, the modified coaxial electrospinning process was conducted to keep the spinneret from clogging for continuous preparation of ibuprofen (IBU)-loaded zein nanofibers, which can provide sustained drug release profiles.

MATERIALS AND METHODS

Materials

Zein was obtained from Aldrich (a purity of 98%, Milwaukee, WI). IBU was purchased from Hubei Biocause Pharmaceutical Co., Ltd (Hubei, China). DMF and anhydrous ethanol was provided by Sinopharm Chemical Reagent Co., Ltd (Shanghai, China). All other chemicals used were of analytical grade, and water was doubly distilled before use.

Modified Coaxial Electrospinning

The core co-dissolving solutions of zein and IBU were prepared by dissolving 30.0 g zein and 3.0 g IBU in 100 mL 80% ethanol aqueous solution (*v/v*). The solutions were degassed with a SK5200H ultrasonicator (350 W; Shanghai Jinghong Instrument Co., Ltd. Shanghai, China) for 30 min before electrospinning.

Two syringe pumps (KDS100 and KDS200, Cole-Parmer, Vernon Hills, IL) and a high-voltage power supply (ZGF 60 kV/2 mA; Shanghai Site Corp., Shanghai, China) were used. The applied voltage was fixed at 14 kV. The nanofibers were collected on an aluminum foil at a distance of 15 cm. All electrospinning processes were carried out under ambient conditions (24±3°C with relative humidity 57±4%) and recorded using a digital video recorder (maximum magnification of ×12, Canon, Tokyo, Japan). A homemade concentric spinneret was used to conduct the modified coaxial electrospinning. The flow rates of the sheath solvent DMF and the core solution are listed in Table I. A traditional single

fluid electrospinning process was also conducted using the homemade concentric spinneret with a zero flow rate of sheath DMF.

Characterization

The morphology of the nanofibers was examined using an S-4800 field emission scanning electron microscopy (FESEM) system (Hitachi, Tokyo, Japan). Prior to the examination, the samples were rendered electrically conductive by gold sputter coating under a nitrogen atmosphere. The average fiber diameter was determined by measuring their diameters in the FESEM images at more than 100 different locations using the Image J software (National Institutes of Health, Bethesda, MD).

Transmission electron microscopy (TEM) images of the samples were recorded on a JEM 2100F field emission transmission electron microscope (JEOL, Tokyo, Japan). TEM samples were collected by fixing a lacey carbon-coated copper grid on the collector.

Differential scanning calorimetry (DSC) analyses were carried out using a MDSC 2910 differential scanning calorimeter (TA Instruments Co., New Castle, DE). Sealed samples were heated at 10°C/min from 20°C to 250°C under a nitrogen flow of 40 mL/min. X-ray diffraction (XRD) patterns were obtained on a D/Max-BR diffractometer (RigaKu, Tokyo, Japan) with CuK α radiation within the 2θ range of 5–60° at 40 mV and 30 mA. Fourier transform infrared (FTIR) analyses were performed on a Nicolet-Nexus 670 FTIR spectrometer (Nicolet Instrument Corporation, Madison, WI) from 500 to 4,000 cm^{-1} at a resolution of 2 cm^{-1} .

In vitro dissolution tests were carried out according to the Chinese Pharmacopoeia (2005 ed.) Method II, a paddle method in which an RCZ-8A dissolution apparatus (Tianjin University Radio Factory, Tianjin, China) was used. About 200 mg of drug-loaded nanofibers were placed in 600 mL of physiological saline (PS; 0.9 wt.%) at 37±1°C. The instrument was then set to 50 rpm, providing sink conditions in which $C < 0.2C_s$. At predetermined time points, 5.0 mL samples were withdrawn from the dissolution medium and replaced with fresh medium to maintain a constant volume. After filtration through a 0.22 μm membrane (Millipore, MA) and appropriate dilution with PS, the samples were analyzed at 272 nm using a UV-vis spectrophotometer (UV-2102PC, Unico Instrument Co. Ltd., Shanghai, China). The cumulative amount of IBU released at each time point was reverse calculated from the data obtained against a predetermined calibration curve. Experiments were carried out six times, and the results are presented as mean values.

RESULTS AND DISCUSSION

The Modified Coaxial Electrospinning Process

A schematic diagram of the modified coaxial electrospinning process with solvent DMF as sheath fluid is shown in Fig. 1a. A homemade concentric spinneret was used to carry out the modified process (Fig. 1b). Two syringe pumps were used to drive the sheath and core fluids independently. The process became a single-fluid electrospinning process when sheath fluid delivery was stopped. An alligator clip was

Table I. Parameters for the Preparation of Fibers and Their Size

No.	Process	Fluid and flow rate (mL/h)		Fiber morphology ^c	Width (μm)
		Sheath fluid ^a	Core fluid ^b		
F1	Single	—	1.0	Ribbon	1.74±0.42
F2	Coaxial	0.1	0.9	Ribbon	0.94±0.34
F3	Coaxial	0.2	0.8	Ribbon	0.67±0.21
F4	Coaxial	0.3	0.7	Spindles-on-a-string	—

^a Sheath fluid is pure DMF

^b Core fluid consists of 30% (*w/v*) zein and 3% (*w/v*) IBU in 80% (*v/v*) ethanol aqueous solutions

^c In this column, “Ribbon” morphology refers to that nanofibers have seldom beads or spindles on them

used to connect the inner stainless steel capillary with the high voltage supply (14, 24).

When single-fluid electrospinning of the core zein/IBU solutions was conducted for preparing fibers F1, the semi-solid “skin” that formed on the nozzle of the spinneret progressively enlarged and made the Taylor cone lose the regular shape, as observed in Fig. 2a–c, until the electrospinning process was totally stopped. The whole process took about 1 min. The semi-solid “skin” needed to be removed manually and frequently to maintain continuity of the electrospinning process.

Figure 2d shows a core/shell droplet formed by the core/sheath fluids themselves in the absence of power when the sheath and core pump were run with a fluid flow rate of 0.2 and 0.8 mL/h, respectively. The sheath DMF well surrounded the core zein and IBU co-dissolving solutions. When a high voltage of 14 kV was applied to the core/sheath fluids, a typical electrospinning process consisting of three stages (Taylor cone, straight fluid jet, and a bending and whipping region) was realized (Fig. 2e). The coaxial electrospinning process proceeded stably and continuously. A compound Taylor cone of the core/sheath fluids is shown in Fig. 2f, where the core solutions gave a deeper color.

In the traditional single fluid electrospinning process, interactions between the spinneret and spinning solutions, as well as the formation of gel-like substances on the spinneret, made spinning inhomogeneous and easy to be interruptive. In stark contrast, spinning is seen to be continuous and homogeneous when using the modified coaxial process, as illustrated in Fig. 1d–f. Clogging is usually thought to occur as a result of the high viscosity of the polymer solution and the usage of high-volatility solvents (13, 16–18). The results reported herein suggest that the situation is more complex and that interactions between the polymer solution and the spinning head also influence the occurrence of clogging.

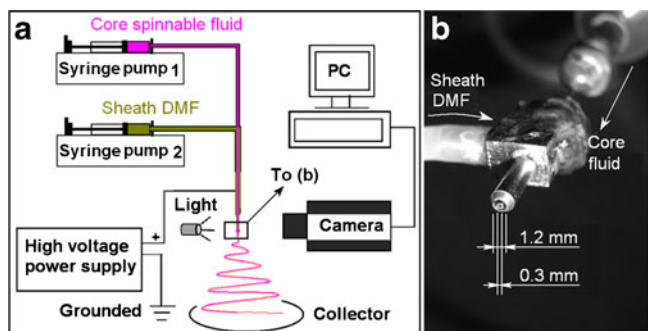


Fig. 1. The modified coaxial electrospinning: **a** schematic diagram of the modified process; **b** the homemade concentric spinneret

Particularly in the present study, zein, as a protein, can easily interact with heavy metal elements in the spinneret through electrostatic interactions and chelation (33). In traditional electrospinning, the applied electrical force needs to be adequate not only to overcome the viscous drag force at the droplet-air interface but also to surpass the drag force from the spinning head: this is crucial to prevent clogging. When the sheath DMF was introduced, interactions between metal elements in the spinning head and the biopolymer in the solution were eliminated. This not only exploited the electrical forces more effectively during electrospinning, but also made it much more difficult for the gel to cling onto the spinning head and thus to clog and interrupt electrospinning.

Morphology and Structure of Nanofibers

FESEM images of the morphology and size distributions of the prepared fibers F1 to F4 are shown in Fig. 3. Fibers F1, F2, and F3 had ribbon morphologies with smooth surfaces and

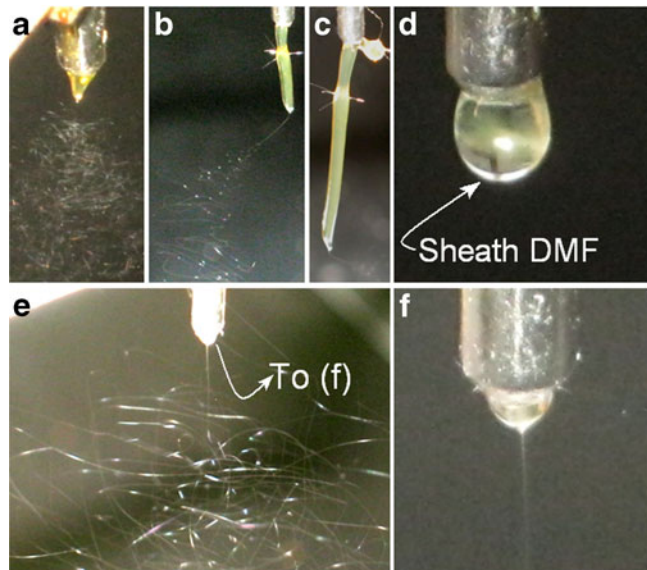


Fig. 2. Observations of the coaxial and single-fluid electrospinning processes: **a–c** The development of clogging in traditional single-fluid electrospinning of the core zein/IBU solution with a deformed Taylor cone; **d** core/shell droplet formed by the core/sheath fluids in the absence of power; **e** typical coaxial electrospinning process under a voltage of 14 kV and flow rates of 0.2 and 0.8 mL/h for the sheath and core fluids, respectively; and **f** a compound Taylor cone of the core/sheath fluids

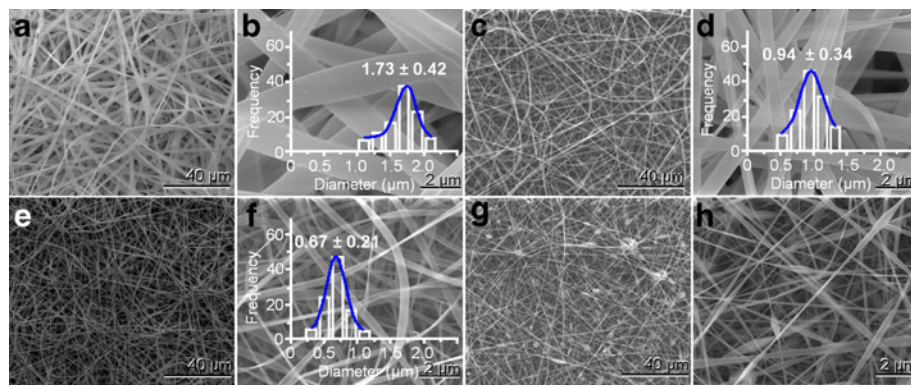


Fig. 3. FESEM images of electrospun nanofibers and their diameter distributions: **a, b** F1; **c, d** F2; **e, f** F3; **g, h** F4

uniform structures and seldom spindles-on-a-string structure. Drug particles on all fiber surfaces resulting from phase separation during the electrospinning process were not observed, which suggested the good compatibility of the filament-forming matrix zein and IBU. The flat ribbon morphology was closely related with the unexpanded β folds of zein whose molecules have a complicated conformation (32). Fibers F1, F2, and F3 had average widths of 1.73 ± 0.42 (Table I; Fig. 3a, b), 0.94 ± 0.34 (Table I; Fig. 3c, d), and 0.67 ± 0.21 μm (Table I; and Fig. 3e, f), respectively. With increased sheath-to-core flow rate ratio, the width of zein/KET nanofibers gradually decreased and its distribution became narrower. This finding can be attributed to the following: (1) the sheath DMF enabling the core electrospinnable fluid jets to be subjected to a long drawing duration under the electrical field (14); and (2) the decrease in exporting total solid solutes from the nozzles of the concentric spinneret. However, excessive sheath solution degraded the coaxial electrospinning process and generated a spindles-on-a-string morphology, as shown in Fig. 3g, h.

The very fast drying electrospinning process, often on the order of 10^{-2} s, can propagate into the solid nanofibers the physical status of the components in the liquid solutions to create the homogeneous nanocomposites (34). Here the sheath DMF could slow down the fast evaporation of solvent in the core fluids and keep them to be subjected to a longer time period drawing before complete drying. Although the total time period was still on the order of 10^{-2} s, it is a concern that if phase separation occurred in the inner part of IBU-loaded fibers. Thus TEM was conducted to observe the nanofiber composites. The TEM images of nanofibers F3 are shown in Fig. 4. The different gray levels along the radial direction of the nanofibers were resulted from the varied thicknesses. The darkest lines at the edge of the under nanofibers were results of enfoldments due to flat ribbon conformation. The gray levels along the axial direction of the nanofibers were similar without any discerned nanoparticles, indicating a homogeneous structure without solid phase separation. Fibers F3 were generated with a larger sheath flow rate (0.2 mL/h) than F1 (0 mL/h) and F2 (0.1 mL/h). This meant that the transformation process from fluid jets to solid fibers for F3 was longer than F1 and F2, leaving more time for possible phase separation in the fibers during the electrospinning. Thus it can be anticipated that fibers F1 and F2 also had a uniform structure as F3.

Physical Status and Compatibility of Components

DSC and XRD tests were performed to determine the physical status of IBU in composite fibers F1 (from the single process), F2, and F3 (from the coaxial process). The DSC thermograms are shown in Fig. 5. The DSC curve of pure IBU exhibited a single endothermic response corresponding to its melting point of 77.3°C ($\Delta H_f = -128.5$ J/g). Being an amorphous polymer, zein did not show any fusion peak or phase transition. The DSC thermograms of the composite fibers F1, F2, and F3 did not show any characteristic peak of IBU, suggesting that IBU was no longer present as a crystalline material and had been converted into an amorphous state in the fiber composites.

As depicted in Fig. 5b, the presence of numerous distinct reflections in the XRD pattern of pure IBU demonstrated that the pure drug was crystalline. The zein diffraction pattern exhibited a diffuse background pattern with two diffraction halos, indicating an amorphous state. In the patterns of fibers F1, F2, and F3, the characteristic reflections of IBU were absent, indicating the amorphous state of the fiber composites, IBU was no longer present as a crystalline material and had been converted into an amorphous state.

The DSC and XRD results both confirmed that IBU was highly distributed in the zein matrix and was present in an amorphous state where the original structure of the pure materials had been lost. These observations concurred with the FESEM and TEM observations, where no separate particles can be discerned on them.

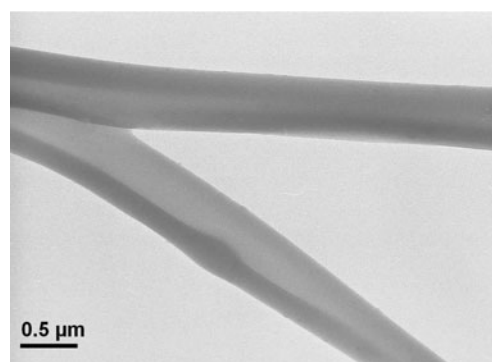


Fig. 4. TEM images of the nanofibers F3

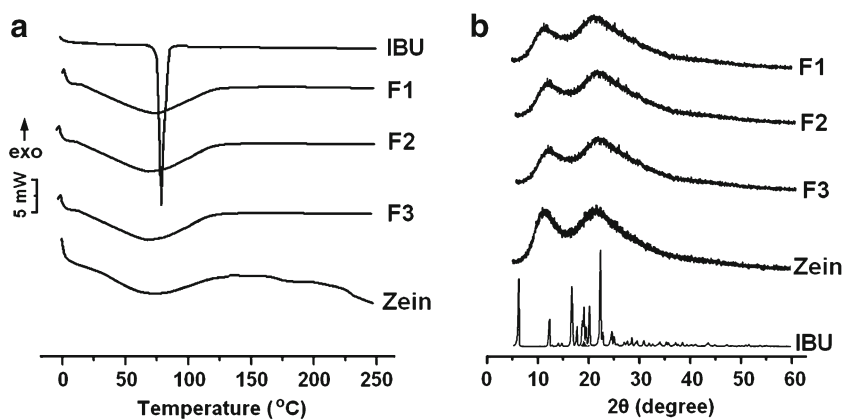


Fig. 5. Physical status characterization: **a** DSC thermograms; **b** XRD patterns

Compatibility among the components is essential in producing high-quality drug-loaded nanofibers, which can be investigated by FTIR analysis (35, 36). Second-order interactions such as hydrogen bonding, electrostatic interactions, and hydrophobic interactions often improve compatibility. IBU and zein molecules possess free hydroxyl groups or amino groups that act as potential proton donors, as well as carbonyl groups that act as potential proton receptors for hydrogen bonding (Fig. 6). Therefore, hydrogen bonding interactions can be speculated to occur within the IBU-loaded zein nanofibers. The FTIR spectra of the components and their nanofibers are shown in Fig. 6. A sharp peak at $1,725\text{ cm}^{-1}$ is visible for pure crystalline IBU due to the stretching of the carbonyl groups. However, this peak was combined with

the stretching of the carbonyl groups in zein and shifted to $1,653\text{ cm}^{-1}$ at the composite fibers F1 and F2. Meanwhile, numerous peaks at the finger region of IBU totally disappeared from the spectra of fibers F1, F2, and F3. These phenomena verify the speculation that hydrogen bonding had taken their roles in the formation of homogeneous composite fibers.

In Vitro Drug Release Profiles

IBU has a UV absorbance peak at 272 nm. Hence, the amount of IBU released from the fibers was determined by UV spectroscopy using a pre-determined calibration curve, $C=13.72A-0.014$ ($R=0.9991$), where C is the IBU concentra-

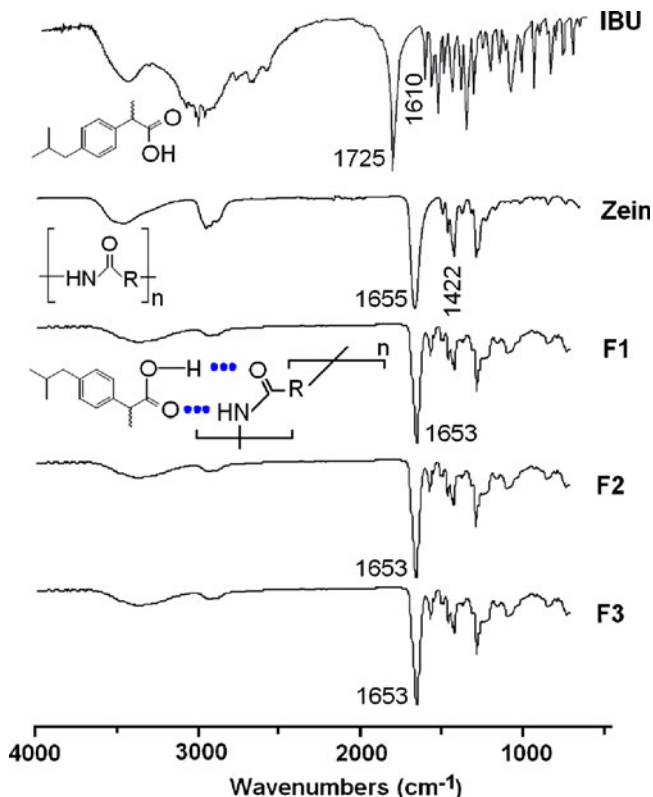


Fig. 6. FTIR spectra of the components (IBU and zein) and their electrospun fibers F1, F2, and F3

tion (in micrograms per milliliter) and A is the solution absorbance at 272 nm (λ_{max} for IBU; linear range, 2–20 $\mu\text{g mL}^{-1}$).

The IBU release profiles of fibers F1, F2, and F3 are shown in Fig. 7. All the three types of fibers had the similar drug sustained release profiles. Fiber F1 prepared by single-fluid electrospinning released 39.6% of the contained drug, indicating an initial burst effect of drug release. Similarly, nanofibers F2 and F3 from the coaxial process released 42.3% and 45.7% in the first hour, respectively, with also obvious initial burst effect. After 6 h of *in vitro* release, fibers F1, F2 and F3 released 88.3%, 94.7%, and 97.1% of the contained IBU, suggesting a similar sustained drug release profile.

To disclose the drug release mechanism, the IBU release profiles were analyzed according to the Peppas equation (37):

$$Q = kt^n$$

where Q is the drug release percentage, t is the release time, k is a constant reflecting the structural and geometric characteristics of fibers and n is the release exponent, which is indicative of the drug release mechanism. The same drug release mechanism was found for all the composite IBU-loaded zein fibers. The equations for F1, F2, and F3 are $Q_1=40.7t^{0.41}$ ($R=0.9951$), $Q_2=44.1t^{0.42}$ ($R=0.9923$), and $Q_3=46.9t^{0.42}$ ($R=0.9961$), respectively. All the values of the release exponent n are less than 0.45, suggesting IBU releases from the three fibers were similarly controlled by a typical Fickian diffusion mechanism.

For drug-loaded fibers, often a larger diameter means a longer distance which the embedded drug must travel if it is to diffuse into the dissolution medium. It is strange here that although fibers F1 have almost two times width of F2 and three times of F3, but the IBU release time periods of F2 and F3 are just slightly shorter than that of F1. This should have a close relationship with the flat ribbon morphology of composite fibers. Although the three types of fibers have significant different widths, their thicknesses might be not so significant. This means that most of the contained IBU in the composite fibers might be free into the dissolution medium through diffusion along the shorter way, *i.e.*, the “thickness” direction, weakening the influence of width on drug release.

Being broken down the traditional concept about coaxial electrospinning that the sheath fluid must be electrospinnable, the modified coaxial process can open a new way in generating novel drug controlled release materials. The unspinnable liquid exploited as sheath fluid in the present study was pure solvent. It can be anticipated that a wide variety of other

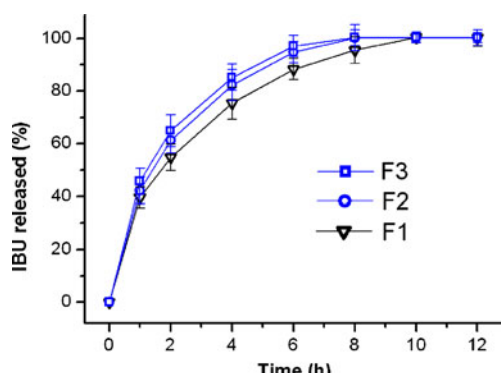


Fig. 7. *In vitro* dissolution profiles of fibers F1, F2, and F3

liquids (such as surfactant solutions, dilute polymer solutions, functional small molecules solutions, suspensions, and also emulsions) may also be exploited as sheath fluids to conduct the modified coaxial process. Thus, the developed process may find its broad applications to generate novel nanostructures for offering new activities, to tailor composition and position of functional ingredients in nanofibers, to process polymer for preparing nanofibers, and to provide new surface modification and functionalization approaches.

CONCLUSIONS

A modified coaxial electrospinning process using only solvent DMF as the sheath fluid was successfully carried out to prepare IBU-loaded zein fibers. The use of DMF as the sheath fluid prevented spinneret-head clogging to smoothen the electrospinning of the core electrospinnable solution enabled the preparation of IBU-loaded zein fibers with finer diameters and narrower diameter distributions. FESEM and TEM images demonstrated that the fibers had ribbon morphology with a smooth surface, as well as average diameters of 0.94 ± 0.34 and $0.67 \pm 0.21 \mu\text{m}$ at sheath-to-core flow rate ratios of 0.11 and 0.25, respectively. XRD and DSC analyses verified that IBU was in an amorphous state in all fiber composites. FTIR spectra showed that zein had good compatibility with IBU because of hydrogen bonding. *In vitro* dissolution tests showed that the drug-loaded fibers could provide sustained drug release files over a time period of 10 h *via* a typical Fickian diffusion mechanism. The modified coaxial electrospinning process reported here expands the capability of electrospinning in generating nanofibers continuously, provides a new approach to develop novel functional nanofiber composites.

ACKNOWLEDGMENTS

We gratefully thank Prof. Deng-Guang Yu for his help in carrying out the modified coaxial electrospinning. This research was supported by the Hubei Provincial Department of Education (Project No. XD20100774), the Hubei Key Laboratory Foundation (Project No. 2012107) and the Natural Science Foundation of Hubei (Project No. 2010CDB05901).

REFERENCES

- Klein S, Kuhn J, Avrahami R, Tarre S, Beliavski M, Green M, et al. Encapsulation of bacterial cells in electrospun microtubes. *Biomacromolecules*. 2009;10:1751–6.
- Xu L, Zheng R, Liu S, Song J, Chen J, Dong B, et al. NiO@ZnO heterostructured nanotubes: coelectrospinning fabrication, characterization, and highly enhanced gas sensing properties. *Inorg Chem*. 2012;51:7733–40.
- Shaikh RP, Pillay V, Choonara YE, du Toit LC, Ndesendo VMK, Bawa P, et al. A review of multi-responsive membranous systems for rate-modulated drug delivery. *AAPS PharmSciTech*. 2010;11:441–59.
- Yu DG, Branford-White C, White K, Li XL, Zhu LM. Dissolution improvement of electrospun nanofiber-based solid dispersions for acetaminophen. *AAPS PharmSciTech*. 2010;11:809–17.
- Brettmann BK, Tsang S, Forward KM, Rutledge GC, Myerson AS, Trout BL. Free surface electrospinning of fibers containing microparticles. *Langmuir*. 2012;28:9714–21.

6. Chiscan O, Dumitru I, Tura V, Stancu A. PVC/Fe electrospun nanofibers for high frequency applications. *J Mater Sci.* 2012;47:2322–7.
7. Brettmann BK, Cheng K, Myerson AS, Trout BL. Electrospun formulations containing crystalline active pharmaceutical ingredients. *Pharm Res.* 2013;30:238–46.
8. Yu M, Sun L, Li W, Lan Z, Li B, Tan L, et al. Investigation of structure and dissolution properties of a solid dispersion of lansoprazole in polyvinylpyrrolidone. *J Mol Struct.* 2011;1005:70–7.
9. Nagy ZK, Balogh A, Vajna B, Farkas A, Patyi G, Kramarics A, et al. Comparison of electrospun and extruded Soluplus® -based solid dosage forms of improved dissolution. *J Pharm Sci.* 2012;101:322–32.
10. Brettmann B, Bell E, Myerson A, Trout B. Solid-state NMR characterization of high-loading solid solutions of API and excipients formed by electrospinning. *J Pharm Sci.* 2012;101:1538–45.
11. Liu X, Lin T, Gao Y, Xu Z, Huang C, Yao G, et al. Antimicrobial electrospun nanofibers of cellulose acetate and polyester urethane composite for wound dressing. *J Biomed Mater Res B Appl Biomater.* 2012;100:1556–65.
12. Liu X, Lin T, Fang J, Yao G, Zhao H, Dodson M, et al. In vivo wound healing and antibacterial performances of electrospun nanofibre membranes. *J Biomed Mater Res.* 2010;94A:499–508.
13. Yu DG, Yu JH, Chen L, Williams GR, Wang X. Modified coaxial electrospinning for the preparation of high-quality ketoprofen-loaded cellulose acetate nanofibers. *Carbohydr Polym.* 2012;90:1016–23.
14. Yu DG, White K, Yang JH, Wang X, Qian W, Li Y. PVP nanofibers prepared using co-axial electrospinning with salt solution as sheath fluid. *Mater Lett.* 2012;67:78–80.
15. Yu DG, Chatterton NP, Yang JH, Wang X, Liao YZ. Coaxial electrospinning with triton X-100 solutions as sheath fluids for preparing PAN nanofibers. *Macromol Mater Eng.* 2012;297:395–401.
16. Kanjanapongkul K, Wongsasulak S, Yoovidhya T. Prediction of clogging time during electrospinning of zein solution: scaling analysis and experimental verification. *Chem Eng Sci.* 2010;65:5217–25.
17. Yu DG, Li X, Wang X, Chian W, Liao Y, Li Y. Zero-order drug release cellulose acetate nanofibers prepared using coaxial electrospinning. *Cellulose.* 2013;20:379–89.
18. Zenis J. Spinning continuous fibers for nanotechnology. *Science.* 2004;304:1917–9.
19. Moghe K, Gupta BS. Co-axial electrospinning for nanofiber structures: preparation and applications. *Polym Rev.* 2008;48:353–77.
20. Yarin AL. Coaxial electrospinning and emulsion electrospinning of core–shell fibers. *Polym Adv Technol.* 2011;22:310–7.
21. Díaz JE, Barrero A, Márquez M, Loscertales IG. Controlled encapsulation of hydrophobic liquids in hydrophilic polymer nanofibers by co-electrospinning. *Adv Funct Mater.* 2006;16:2110–211.
22. Yu DG, Wang X, Li X, Chian W, Li Y, Liao Y. Electrospun biphasic drug release polyvinylpyrrolidone/ethyl cellulose core/sheath nanofibers. *Acta Biomater.* 2013;9:5665–72.
23. Samarasinghe SR, Balasubramanian K, Edirisinghe MJ. Encapsulation of silver particles using co-axial jetting. *J Mater Sci Mater Electron.* 2008;19:33–8.
24. Yu DG, Williams GR, Gao LD, Bligh SWA, Yang JH, Wang X. Coaxial electrospinning with sodium dodecylbenzene sulfonate solution for high quality polyacrylonitrile nanofibers. *Colloids Surf A Physicochem Eng Aspect.* 2012;396:161–8.
25. Yu DG, Lu P, Branford-White C, Yang JH, Wang X. Polyacrylonitrile nanofibers prepared using co-axial electrospinning with LiCl solution as sheath fluid. *Nanotechnology.* 2011;22:435301.
26. Yu DG, Yang JM, Li L, Lu P, Zhu LM. Obtaining finer polymer nanofibers using two different electrospinning processes. *Fiber Polym.* 2012;13:450–5.
27. Lai LF, Guo HX. Preparation of new 5-fluorouracilloaded zein nanoparticles for liver targeting. *Int J Pharm.* 2011;404:317–23.
28. Torres-Giner S, Ocio MJ, Lagaron JM. Novel antimicrobial ultrathin structures of zein/chitosan blends obtained by electrospinning. *Carbohydr Polym.* 2009;77:261–6.
29. Tiwari SK, Tzezana R, Zussman E, Venkatraman SS. Optimizing partition-controlled drug release from electrospun core-shell fibers. *Int J Pharm.* 2010;392:209–17.
30. Jiang HL, Zhao PC, Zhu KJ. Fabrication and characterization of zein-based nanofibrous scaffolds by an electrospinning method. *Macromol Biosci.* 2007;7:517–25.
31. Jiang QR, Reddy N, Yang YQ. Cytocompatible crosslinking of electrospun zein fibers for the development of waterstable tissue engineering scaffolds. *Acta Biomater.* 2010;6:4042–51.
32. Nie W, Yu DG, Branford-White C, Shen XX, Zhu LM. Electrospun Zein/PVP fiber composite and its application in drug delivery. *Mater Res Innov.* 2012;16:14–8.
33. Blundell TL, Jenkins JA. The binding of heavy metals to proteins. *Chem Soc Rev.* 1977;6:139–71.
34. Li D, Xia Y. Electrospinning of nanofibers: Reinventing the Wheel? *Adv Mater.* 2004;16:1151–70.
35. Yu DG, Zhu LM, Branford-White C, Yang JH, Wang X, Li Y, et al. Solid dispersions in the form of electrospun core-sheath nanofibers. *Int J Nanomedicine.* 2011;6:3271–80.
36. Woods KK, Selling GW, Cooke PH. Compatible blends of zein and polyvinylpyrrolidone. *J Polym Environ.* 2009;17:115–22.
37. Peppas NA. Analysis of Fickian and non-Fickian drug release from polymers. *Pharm Acta Helv.* 1985;60:110–1.